Available online at www.sciencedirect.com
SCIENCE DIRECT®
Journal of Photochemistry and Photobiology A: Chemistry 162 (2004) 81–88
Journal of Photochemistry and Photobiology A:Chemistry
www.elsevier.com/locate/jphotochem

Photo-oxidation of tertiary amides, main degradation products of large malonamides

Franck Delavente [a], Jean-Michel Guillot [a,*], Olivier Thomas [a], Laurence Berthon [b], Christine Nicol [b]

[a] *Ecole des Mines d'Alès, LGEI, F-30319 Alès, France*
[b] *CEA Valrho Marcoule, DEN/DRCP/SCPS/LCSE, Bat 399, F-30207 Bagnols/Cèze, France*

Received 3 June 2003; received in revised form 23 June 2003; accepted 26 June 2003

Abstract

Photo-oxidation of large malonamides *N*,*N*′-dimethyl, *N*,*N*′-dibutyl, tetradecyl malonamide (DMDBTDMA) and *N*,*N*′-dimethyl, *N*,*N*′-dibutyl, dodecylethoxy malonamide (DMDBDDEMA)—potential extractants for minor actinides in nuclear fuel reprocessing—leads mainly to the corresponding monoamides: *N*-butyl *N*-methyl hexadecanamide (BMHDA) and *N*-butyl *N*-methyl dodecyl oxy butanamide (BMDDOBA), respectively. The evolution of these main photoproducts was monitored during the degradation of malonamide solutions, and also pure monoamide solutions. Irradiation, for 1 h, with a low mercury pressure lamp can destroy BMHDA when diluted to 0.075 mol l^{-1} in *n*-dodecane. The two monoamides only differ by an ether bond and the weakness introduced by such a function in an alkyl chain is shown by slightly faster degradation. The relative weakness of BMDDOBA is independent of oxidant addition. Global degradation can be monitored by GC/FID or UV detection at 200 nm.

Keywords: Photodegradation; Tertiary amide; Diamide; Oxidation

1. Introduction

The management of radioactive wastes produced after spent nuclear fuel reprocessing is based on separation processes. In this field, a development made by the Commissariat à l'Energie Atomique (CEA) consists in separating the minor actinides (Am(III) and Cm(III)) from the high level liquid waste. A first step in the separation strategy, the DIAMEX process (with incinerable malonamide extractants made only with C, H, O, and N atoms) is the extraction of trivalent minor actinides and lanthanides. The typical diamide showing DIAMEX process feasibility is DMDBTDMA (*N*,*N*′-dimethyl, *N*,*N*′-dibutyl tetradecyl malonamide: $(C_4H_9(CH_3)NCO)_2CH(C_{14}H_{29})$) [1]. Another similar diamide, differing only in having an ether bond in the main alky chain, was also monitored: DMDBDDEMA (*N*,*N*′-dimethyl *N*,*N*′-dibutyl dodecyloxyethyl malonamide: $((C_4H_9(CH_3)NCO)_2CH(C_2H_4OC_{12}H_{25}))$. The hostile environment of the extraction process (concentrated acid, high radiation) can lead to partial degradation of the extractant [2] and all information about cleanup procedures to remove by-products and degradation pathways must be obtained by studying diamides or the main photoproducts, which are monoamides: *N*-butyl *N*-methyl hexadecanamide (BMHDA) and *N*-butyl *N*-methyl dodecyl oxy butanamide (BMDDOBA). The respective semi-developed formulae of the malonamides and monoamides are:

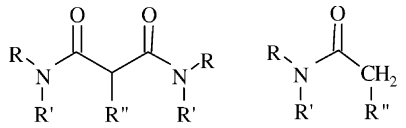

where R, R′ and R″ are alkyl or oxyalkyl groups [3–6].

Previous studies had been carried out on the thermal destruction of tertiary monoamides [7,8] and malonamides [9]. Photo-oxidation of these malonamide extractants had also been studied [10]. This paper deals with the photo-oxidation of monoamides: BMHDA and BMDDEMA, the comparison between these structures and the influence of different factors such as the irradiation device used, and the concentration or presence of oxidant.

* Corresponding author. Tel.: +33-4-66-78-2780; fax: +33-4-66-78-2701.
E-mail address: jean-michel.guillot@ema.fr (J.-M. Guillot).

1010-6030/$ – see front matter © 2004 Elsevier B.V. All rights reserved.
doi:10.1016/S1010-6030(03)00314-9

2. Experimental

2.1. Materials and apparatus

2.1.1. Compounds

Diamides (malonamides) and monoamides (tertiary amides) were synthesised by Panchim (Evry, France) with purity up to 99%. Solutions were prepared by dilution in pure *n*-dodecane (Acros, 99). For CG/FID analysis, hexadecane (Fluka, [JB1] 98%) was added to samples as internal standard (I.S.). The developed formulae of the diamides DMDBTDMA and DMDBDDEMA are as follows:

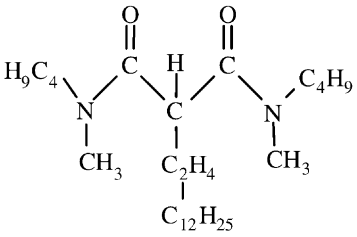

DMDBTDMA

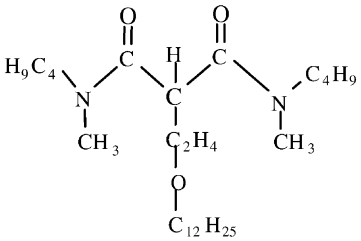

DMDBDDEMA

The developed formulae of the monoamides, *N*-butyl *N*-methyl, hexadecanamide (BMHDA) and *N*-butyl *N*-methyl, dodecyloxobutylamide (BMDDOBA) are as follows:

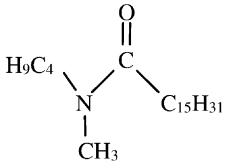

BMHDA

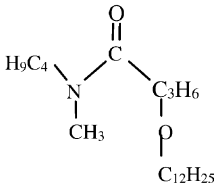

BMDDOBA

2.1.2. Irradiation devices and low pressure mercury lamps

Irradiation was carried out using an UVP Pen-Ray mercury lamp (25 W) or a NIQ 48 Heraus mercury lamp (100 W). Details of devices and lamp emission spectra are described in a previous paper [10].

2.2. Photolysis experiments

2.2.1. Absorbance evolution for diamides and monoamides solutions

0.5 mol l^{-1} solutions were irradiated for 400 min using the UVP device. UV spectra were recorded for diluted solutions (with a dilution factor of 500 times, i.e. a concentration of 1 mmol l^{-1} for initial solutions). These spectra were obtained with a Secomam spectrophotometer, bandwith 2 nm, scanspeed 1800 nm min^{-1}, 2 mm pathlength quartz cell.

2.2.2. Identification of photo-products

Monoamide by-products were analysed by both the GC/MS and the GC/FTIR devices, and quantified by means of GC/FID. All chromatographic conditions were developed for the monitoring of thermal degradation experiments and are given in [9].

2.2.3. Photo-oxidation of 0.5 mol l^{-1} solutions

Experiments were carried out with UVP Device, on both monoamides at 0.5 mol l^{-1} in *n*-dodecane.

2.2.4. Comparison between BMHDA and BMDDOBA solutions

The influence of the lamp device on degradation was studied by means of experiments on both monoamides and with both lamps.

2.2.5. Influence of monoamide solution concentration

Solutions of BMHDA at 0.5, 0.075, and 0.0075 mol l^{-1} in *n*-dodecane were tested with the Heraus device to investigate the influence of concentration.

2.2.6. Influence of oxidant on BMDDOBA degradation

Solutions of BMDDOBA 0.075 mol l^{-1} in *n*-dodecane treated with hydrogen peroxide (saturation of initial solution) or with oxygen (2 ml min^{-1} O_2 flow rate in the solution) were compared with an untreated solution (dry solution).

2.2.7. Comparison of GG-FID and UV detection

A solution of BMDDOBA at 0.075 mol l^{-1} in *n*-dodecane was degraded using the Heraus device for 200 min. Samples at different times were collected and analysed by GC/FID and the Global Residual Percentage (GRP) was calculated using the chromatogram data. During the same experiments, the circulation of the solution in the device was coupled with the UV spectrophotometer used as an on-line detector.

2.3. Destruction indicators

Destruction was monitored by means of GC/FID or UV detection.

With GC/FID, two indicators were obtained: the FID Residual Percentage (FIDRP) and the Global Residual Percentage (GRP). FIDRP is the ratio of the sum, at time *t*, of FID signals for all detected compounds (excepted Internal Standard (I.S.) and *n*-dodecane) divided by the area of I.S. and the same expression at time 0. Such an indicator takes into account the relative evolution of the response coefficient of all organic compounds and therefore provides

an indication of degradation and oxidation too, because the FID response decreases with the oxidation degree of a carbon atom. GRP is based on the conversion ratio T_i of the initial diamide in product i, taking into account molecular weights. The relations give the FIDRP and GRP calculation:

$$\text{FIDRP} = 100 \times \frac{\left(\sum \text{Areas} - A_{\text{I.S.}} - A_{\text{dodecane}}\right)_t / -(A_{\text{I.S}})_t}{\left(\sum \text{Areas} - A_{\text{I.S.}} - A_{\text{dodecane}}\right)_0 / -(A_{\text{I.S}})_0}$$

where $\sum$ Areas is the sum of FID signals for detected compounds, $A_{\text{I.S.}}$ the FID response for internal standard (hexadecane), A_{dodecane} the FID response for solvent (*n*-dodecane), t is the time.

$$\text{GRP} = \sum_i \left(\frac{M_i}{M_{\text{d}}}\right) T_i$$

where M_i is the molecular weight of molecule i, M_{d} the molecular weight of initial diamide, T_i the ratio (moles of molecule i/moles of initial diamide), when T_i was lower than 1%, such a conversion was not included in the calculation.

UV detection was performed between 200 and 220 nm. Absorbance was normalized as a percentage of initial solution absorbance.

3. Results and discussion

3.1. Absorbance evolution for diamide and monoamide solutions

The absorbance of diamide and monoamide solutions, at 1 mmol l^{-1} in *n*-dodecane, is given in Figs. 1 and 2. The evolution of the absorbance for both diamides and both monoamides indicates transformation of these molecules. For diamides, the absorption decreases in the range 200–220 nm and increases between 230 and 250 nm. Such an evolution of spectra was also observed with monoamide spectra.

3.2. Identification of photo-products

The identification performed by CG/MS and CG/FTIR showed several kinds of compounds. A major part of these by-products were amides (Table 1). Lower tertiary amides were obtained by the loss of some carbons on the *C*-alkyl or *C*-oxo-alkyl chain and secondary amides were obtained by cleavage of an *N*-alkyl group. Several formamides and some aldehydes or carboxylic acids due to oxidation of long *C*-alkyl fragments were also obtained. Cleavages of *N*-alkyl bonds (methyl or butyl) were due to the hydrogen lability of Cα–H. Globally, photo-degradation of both monoamides led to similar structures due to the same mechanisms being involved.

3.3. Photo-oxidation of solutions at 0.5 mol l^{-1}

Photo-oxidation of diamide DMDBTDMA was more efficient than for its monoamide BMHDA (Fig. 3). The kinetic constant for kinetic curve tendency was five times lower for the monoamide than for the diamide. The diamide is a larger molecule, therefore, more bonds can be cleaved, and the malonamide structure may also introduce a weakness into the molecule as compared with the mono tertiary amide, explaining the different kinetics. This last hypothesis is confirmed looking at the conversion of DMDBTDMA to BMHDA, which is typically due the lost of malonamide structure without cleavages for *N*-alkyl groups. The global degradation shown by FIDPR values confirms that the diamide is less stable than its homologous monoamide.

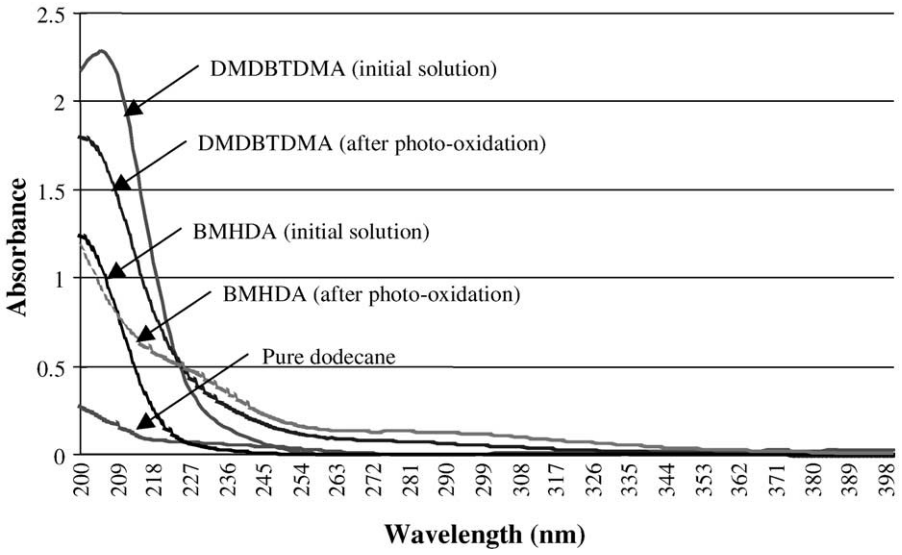

Fig. 1. UV spectra for initial and degraded solutions of DMDBTDMA and BMHDA (initial concentration of amide: 0.001 mol l^{-1} in *n*-dodecane, 400 min irradiation time with UVP device).

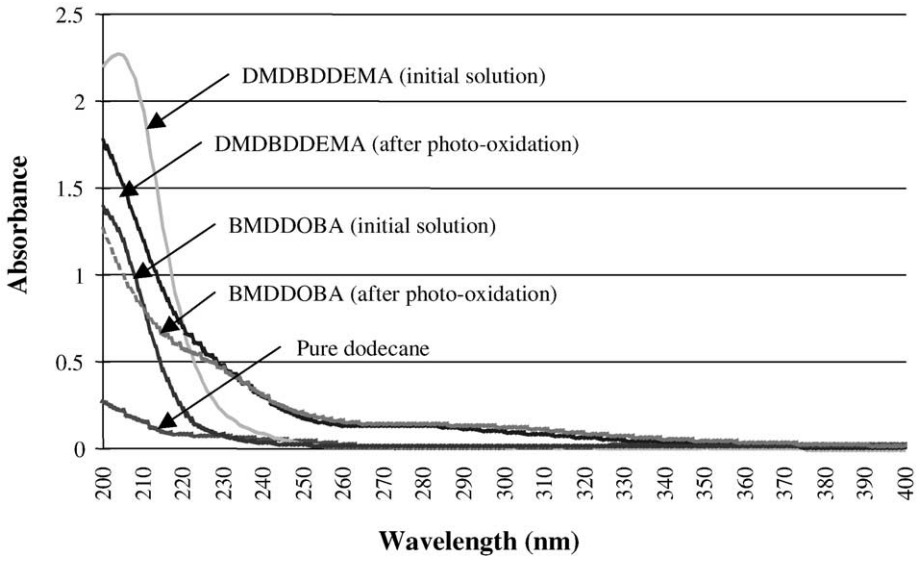

Fig. 2. UV spectra for initial and degraded solutions of DMDBDDEMA and BMDDOBA (initial concentration of amide: 0.001 mol l^{-1} in *n*-dodecane, 400 min irradiation time with UVP device).

Table 1
Main amide structures (and molecular weights) for both monoamides photoproducts

Initial tertiary amide	BMHDA (325)	BMDDOBA (341)
Lower tertiary amides		
Cleavage of a part of longer alkyl chain	R″ $CON(CH_3)C_4H_9$ R″ ≤ C7 alkyl chain	R″ $OC_3H_6CON(CH_3)C_4H_9$ R″ ≤ C11 alkyl chain
Secondary amides		
Cleavage of *N*-methyl group	$C_{15}H_{31}CONHC_4H_9$ (311)	$C_{12}H_{25}OC_3H_6CONHC_4H_9$ (327)
Cleavage of *N*-butyl group	$C_{15}H_{31}CONHCH_3$ (269)	$C_{12}H_{25}OC_3H_6CONHCH_3$ (285)
Disubstituded formamide		
Cleavage of the longer alkyl chain	$HCON(CH_3)C_4H_9$ (115)	
Other formamides		
Cleavages of the longer alkyl chain and *N*-methyl group	$HCONHC_4H_9$ (101)	
Cleavages of the longer alkyl chain and *N*-butyl group	$HCONHCH_3$ (59)	
Cleavages of all substitutants	$HCONH_2$ (45)	

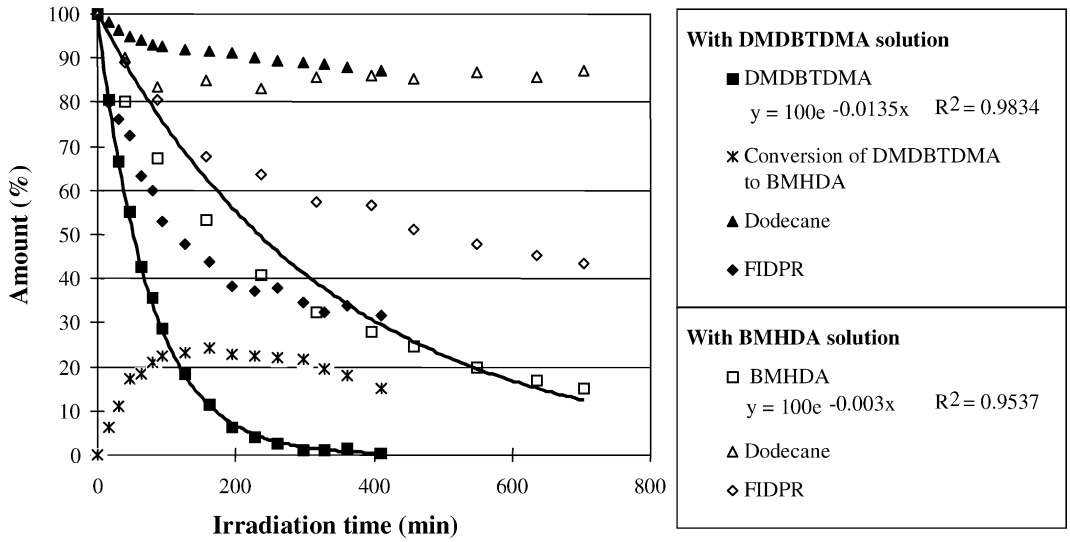

Fig. 3. Photo-oxidation of 0.5 mol l^{-1} solutions of DMDBTDMA and BMHDA in *n*-dodecane.

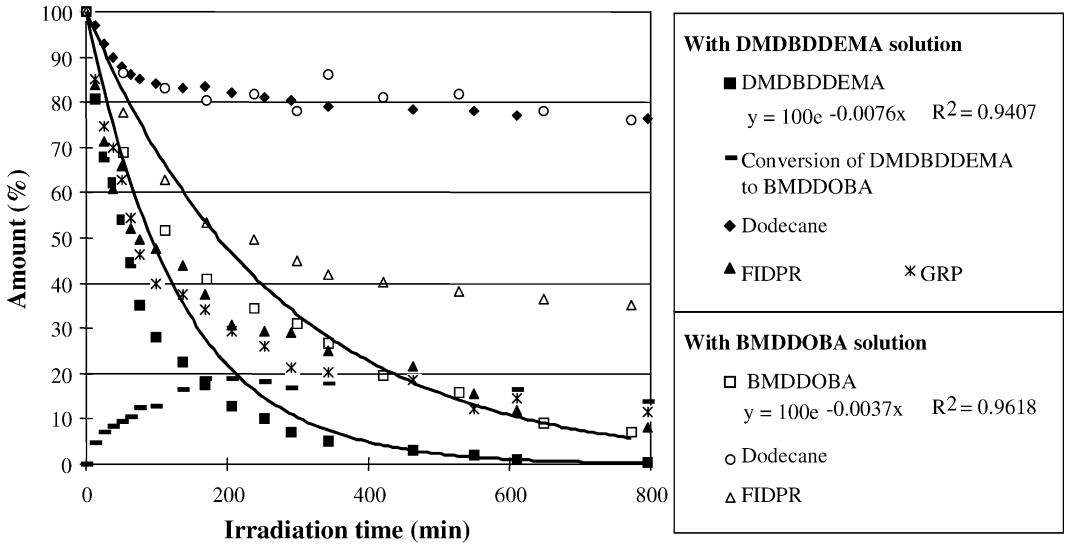

Fig. 4. Photo-oxidation of 0.5 mol l^{-1} solutions of DMDBDDEMA and BMDDOBA in *n*-dodecane.

The same behaviour is observed in Fig. 4 for the diamide/monoamide couple with the ether bond (DMDBDDEMA and BMDDOBA). The difference between diamide and monoamide behaviour is less important than for the previous couple. These structures with ether bonds are globally stable, like their homologue without oxygen in the aliphatic chain. Bonds in the α position of the amide group are easily broken in diamide structures [10,11]. The global degradation observed with FIDPR follows the same tendency as for the previous couple. For diamide, quantification by GRP calculation was very close to the global FID response (FIDPR) showing that this last indicator can give precise information about the degradation pathway.

For both monoamides and both diamides, the degradation of *n*-dodecane is at a rate of 15–25% for a 600 min irradiation time (Figs. 3 and 4).

3.4. Comparison between BMHDA and BMDDOBA solutions

Photo-degradation of monoamides led to very similar degradation behaviour, as shown in Fig. 5. Both monoamides have the same evolution even if BMDDOBA is a little weaker than BMHDA because of its ether bond. Looking at the FIDPR, which takes into account all organic compounds detected with GC/FID analysis, this reactivity is

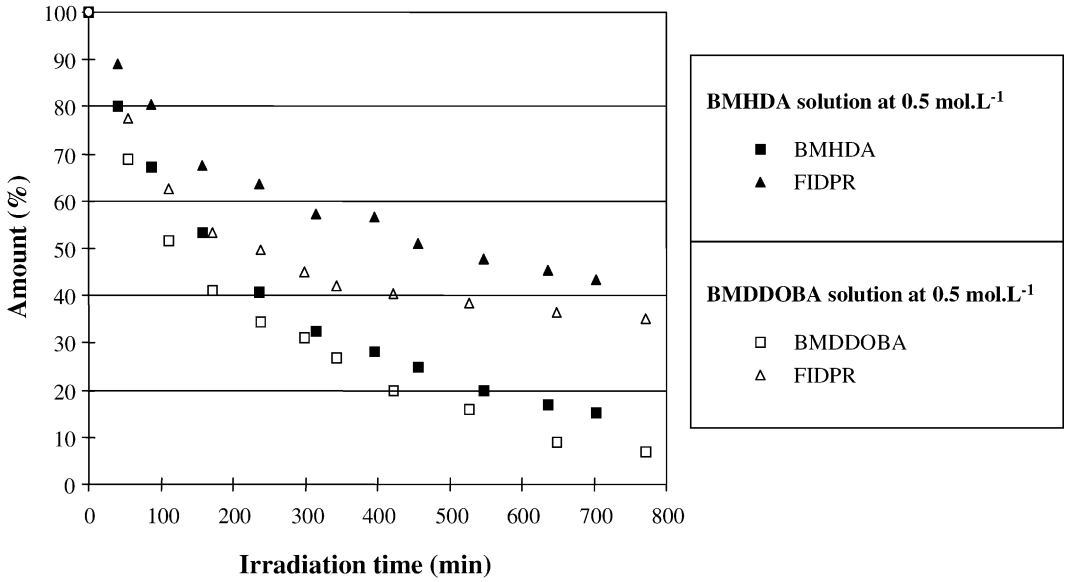

Fig. 5. Photo-oxidation of 0.5 mol l^{-1} in *n*-dodecane solutions of both monoamides with UVP device.

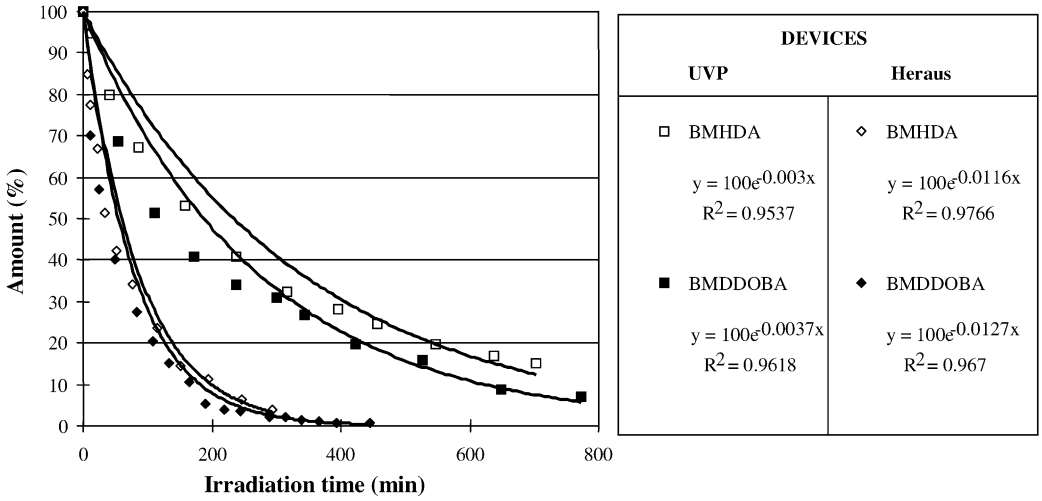

Fig. 6. Photo-oxidation of both 0.5 mol l^{-1} monoamide solutions in *n*-dodecane with UVP and Heraus devices.

most clearly shown because some BMDDOBA by-products (parts of oxo-alkyl chain) can be photo-oxidised quickly.

3.5. Photo-oxidation of monoamide solutions with two devices

The degradation efficiency of the two lamps (Heraus and UVP) was compared for solutions at 0.5 mol l^{-1} as shown in Fig. 6. These experiments clearly show the higher monoamide degradation efficiency of the Heraus device compared to the UVP device. For both devices, DMDDOBA was always degraded quickly because of the reactivity of its ether bond. Such a difference is quite independent of the device when the DMDDOBA/BMHDA ratios of kinetic constants are compared. These ratios are 1.1 (0.0127/0.0116) and 1.2 (0.0037/0.003) for the Heraus and UVP devices, respectively.

3.6. Influence of monoamide solution concentration

The influence of concentration on BMHDA is shown in Fig. 7. On the one hand, these results indicate that the limiting factor for degradation is the radiation from the lamp, and with high concentration, the large amount of initial molecule cannot be destroyed at was shown for DMDBTDMA malonamide [10]. On the other hand, with very low concentration, the degradation increase is not as strong as had been estimated, as can be seen from the lower kinetic constant ratio K_3/K_1 than concentration ratio C_1/C_3 in Table 2.

Table 2
Comparison between BMHDA concentration and degradation kinetic constant ratios

Concentration (mol l^{-1})	Kinetic constant (s^{-1})	Concentration ratio	Kinetic constant ratio
$C_1 = 0.5$	$K_1 = 0.0116$	$C_1/C_3 = 66.7$	$K_3/K_1 = 42.2$
$C_2 = 0.075$	$K_2 = 0.0714$	$C_1/C_2 = 6.7$	$K_2/K_1 = 6.2$
$C_3 = 0.0075$	$K_3 = 0.489$	$C_2/C_3 = 10$	$K_3/K_2 = 6.8$

3.7. Influence of oxidant on BMDDOBA degradation

The influence of the two oxidants on BMDDOBA degradation is illustrated by Fig. 8. The dry solution at 0.075 mol l^{-1} (only monoamide in *n*-dodecane) was

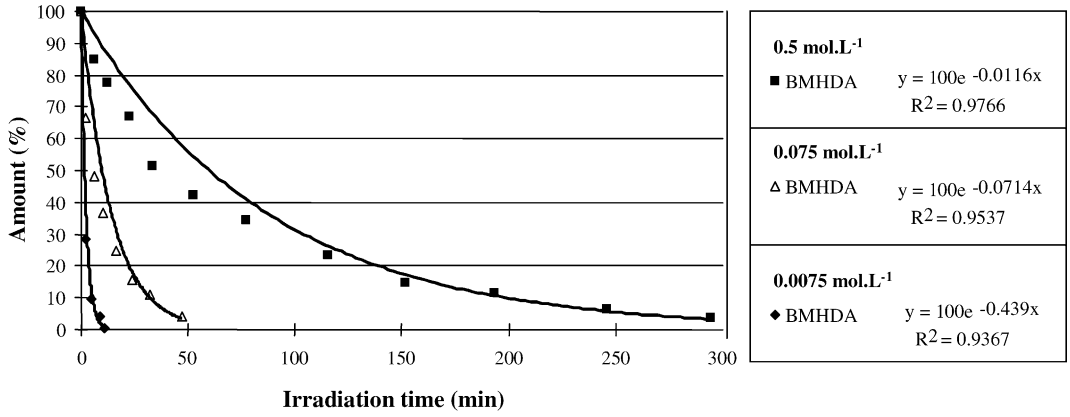

Fig. 7. Photo-oxidation of 0.5, 0.075 and 0.0075 mol l^{-1} solutions of BMHDA in *n*-dodecane with Heraus device.

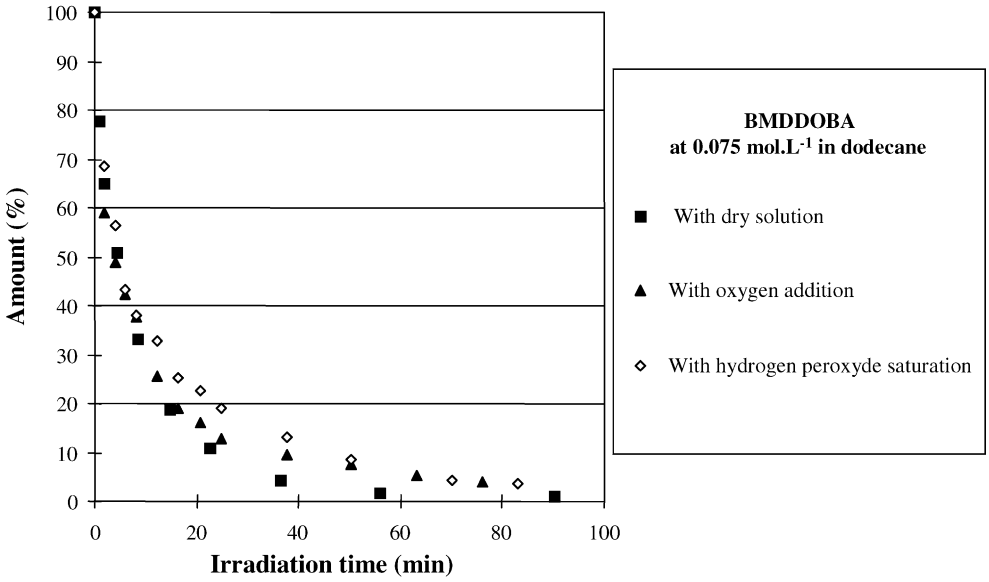

Fig. 8. Influence of oxidant addition on DMDDOBA photo-oxidation.

compared with similar solutions containing hydrogen peroxide or permanent introduced oxygen. No significant difference was observed with these three solutions, indicating that degradation is not accelerated by the presence of these oxidants.

3.8. Comparison of GG-FID and UV detection

A comparison of the two ways of monitoring monoamide degradation is shown in Fig. 9. The GRP calculated with FID data shows a complete degradation of monoamide and main by-products after 200 min irradiation time. The direct UV measurement is less precise because the relative absorbance between 200 and 220 nm decreases by just 50%, but is more convenient. The residual absorbance is due to low-level [JB2] by-products and the solvent. All points for GRP were obtained after sampling and three injections in CG/FID while UV values are given in real time. The efficiency of UV is shown and can be completed with the increase of absorbance in the range 271–276.3 nm. In such

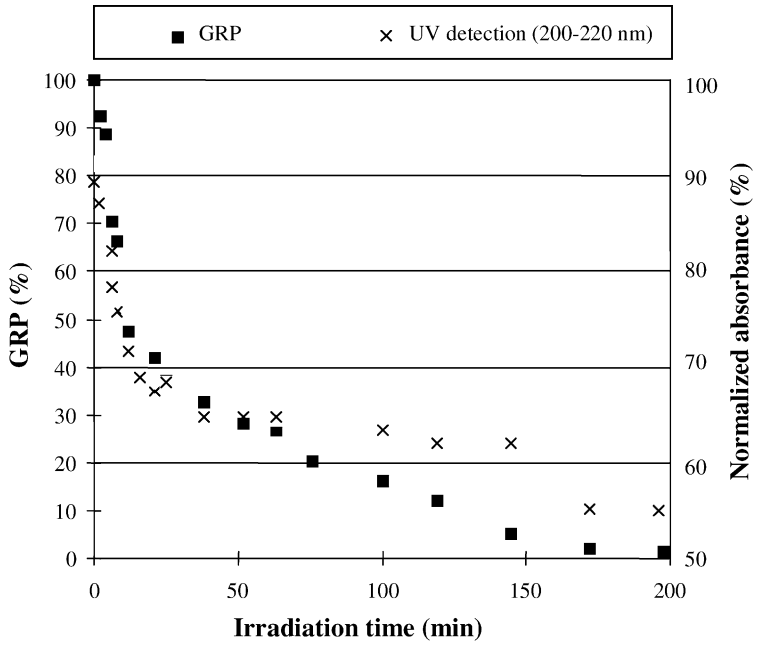

Fig. 9. Comparison of normalized absorbance decrease at 200 nm with global FID quantification (GRP) for BMDDOBA photo-degradation.

a range, relative absorbance starts from 0 to 100% with 120 min irradiation time and then decreases. This last range can be useful to monitor the beginning of the degradation and the formation of the first by-products but cannot be maintained for monitoring the global degradation.

4. Conclusion

The photo-degradation of monoamides was carried out under different conditions. Their degradation was compared to malonamide degradation. These malonamides are in fact precursors of the studied monoamides in a complex degradation pathway. Monoamide structures BMHDA and BMDDOBA are more stable than their respective malonamides DMDBTDMA and DMDBDDEMA under the same photo-degradation conditions. The ether bond in the large alkyl chain introduces a weakness because BMDDOBA is degraded more quickly than BMHDA. The device comparison showed that the Heraus system is more efficient than the UVP one. Monoamide degradation is low with concentrated solutions because the emission of the lamps is limited, but with diluted solutions ($0.0075\,\mathrm{mol\,l^{-1}}$), this degradation takes less than 30 min and the addition of oxidant does not seem to modify the degradation. The global degradation of these tertiary amides was carried out using several indicators based on the CG/FID response and UV detection. The Global Residual Percentage (GRP) or the FID Residual Percentage (FIDRP) can give precise information about the destruction, taking into account not only the decrease in initial molecule but also the evolution of the main detected by-products. This destruction can be monitored easily by means of direct UV detection when a spectrophotometer is coupled to the photo-degradation device.

Acknowledgements

This work was carried out at the “Ecole des Mines d’Alès” in the framework of a CEA-Valrho (Marcoule-FRANCE) research project.

References

[1] C. Madic, P. Blanc, N. Condamines, P. Baron, L. Berthon, C. Nicol, C. Pozo, M. Lecomte, M. Philippe, M. Masson, C. Hequet, M.J. Hudson, in: Proceedings of the International Conference Recod’94, London, April 1994.
[2] L. Berthon, J.M. Morel, N. Zorz, C. Nicol, H. Virelizier, C. Madic, Sep. Sci. Technol. 36 (5–6) (2001) 709–728.
[3] L. Nigond, Ph.D. thesis, University Clermont-Ferrand II and CEA Report R5610, 1992.
[4] L. Nigond, N. Condamines, P.Y. Cordier, J. Livet, C. Madic, C. Cuillerdier, C. Musikas, M.J. Hudson, Sep. Sci. Technol. 30 (1995) 2075–2099.
[5] C. Madic, M.J. Hudson, Report Eur 18038, 1998.
[6] C. Madic, M.J. Hudson, J.O. Liljenzin, J.P. Glatz, R. Nannicini, A. Facchini, Z. Kolarik, R. Odoj, Report Eur 19149, 2000.
[7] T. Dagnac, J.M. Guillot, P. LeCloirec, J. Anal. Appl. Pyrolysis 37 (1996) 33–47.
[8] T. Dagnac, J.M. Guillot, P. LeCloirec, J. Anal. Appl. Pyrolysis 42 (1997) 53–71.
[9] F. Delavente, J.M. Guillot, O. Thomas, L. Berthon, C. Nicol, J. Anal. Appl. Pyrolysis 58–59 (2000) 589–603.
[10] F. Delavente, J.M. Guillot, O. Thomas, L. Berthon, C. Nicol, J. Photochem. Photobiol A: Chem. A 158 (2003) 55–62.
[11] W.H. Sharey, W.E. Mochels, J. Am. Chem. Soc. 81 (1959) 3000–3005.